Global Dynamics of terrestrial planets in ESPs

R. Dvorak[1], E. Pilat-Lohinger[1], R. Schwarz[1], B. Funk[1], Z. Sándor[2], B. Érdi[2], A. Süli[2]

1: Institute for Astronomy - University of Vienna, 2 : Department of Astronomy, Eötvös University, Budapest

Introduction

Today any research for possible additional planets of the size comparable to the earth is a hypothetical one. This doesn' t mean that extrasolar planetary systems were not able to form less massive, terrestrial planets. Indeed, as opposed to Jupiter in our solar system, the gravitational zone of influence of the extrasolar giant planets often approaches, or sometimes even overlaps with, the habitable zone. There are different possible regions where a 'terrestrial planets' in a distance called "habitable zone", could have (a) liquid water on its surface and (b) a stable atmosphere:

1) When the gas giant is very close to the star from the dynamical point of view there exist stable orbits in the habitable zone with sufficiently small eccentricities over time scales long enough to develop a biosphere.

2) When this planet moves far enough from its central star to allow additional planets moving on stable low eccentic orbits closer to the star - like in our Solar System.

3) When the gas giant itself moves in the habitable region a terrestrial satellite (as the ones orbiting Jupiter) could have the right conditions to develop a biosphere.

4) When the gas giant moves in the habitable region a terrestrial Trojan planet may move on a stable orbit around the Lagrangian equilibrium points L_4 or L_5, which could have the right conditions to develop a biosphere.

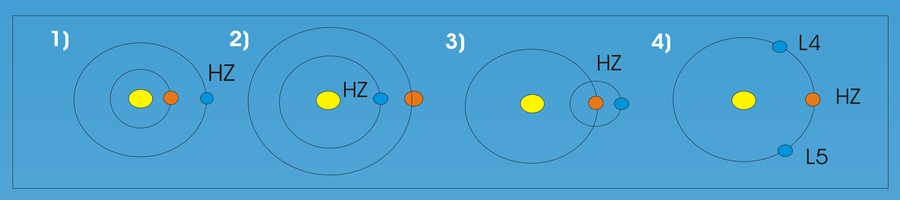

We have chosen two complementary numerical methods to answer the question of the largeness of the stability region; both use direct numerical integrations of the equations of motion. As a first approach we did the computations in the dynamical model of the spatial elliptic restricted three body problem consisting of the central star and the gas giant as massive bodies and a massless hypothetical terrestrial planet moving in the gravitational field of the two masses.

The 2 integration methods were the LIE-integration and the Burlirsch-Stoer integration; both with an adaptive step size.

As methods of analysis we used

(i) the Fast Lyapunov Indicators (FLI): The Fast Lypunov Indicator (FLI) measures the length of the largest tangent vector (psi(t)= sup_i ||v_i(t)||, where i =1, ... n and n denotes the dimension of the phase space= and is therefore a fast method to distinghuish between regular and chaotic behaviour. It was introduced by Froeschle et al. in 1997. The computation time depends on the investigated system and is in general between 1000 and 100000 times of the longest orbital period.

(Ii) the maximum eccentricity method (MEM): This method provides the value of the largest eccentricity (e) of the orbit, which is also an indicator for the variation of the temperature between periastron and apoastron which should not be too large -we estimate that e < 0.2 during the integration time is a reasonable choice.

(Iii) the relative Lyapunov Indicators (RLI): The Relative Lypunov Indicator (RLI) measures the convergence of the finite time Lyapunov indicators to the maximal Lyapunov characteristic exponents of two very close orbits. This method is extremely fast to determine the ordered or chaotic nature of orbits. It was introduced by Sandor et al. in 2000. The computation time for the RLI is a few hundered times of the longest orbital period of the investigates system.

Stability catalogue for Trojan planets

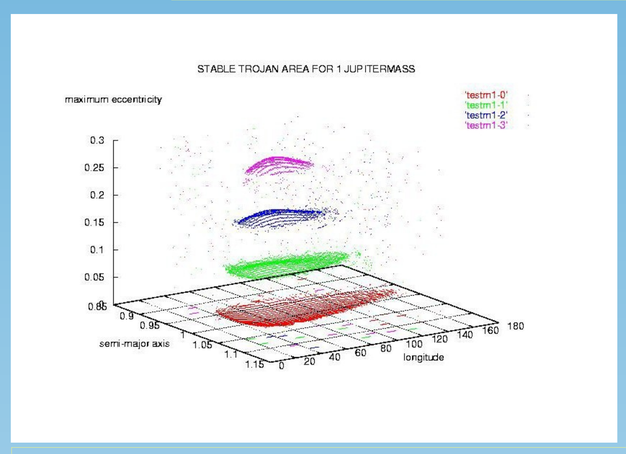

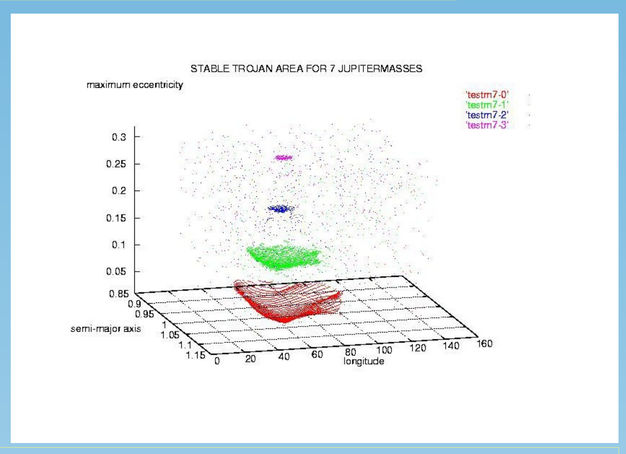

Figure 1: Trojanercatalogue (elliptic three body problem): Dependance of the stable region around the Lagrange point L4. For a fine grid in semimajor axis (0.85 < a < 1.15 with delta a = 0.01 AU) and in the angular distance of the Lagrange point (0 < l < 180 with delta l = 1 degree) with different initial eccentricities of the primary's orbit (0, 0.05, 0.1, 0.15) the stable area was determined via numerical integrations. The initial diagramm plot 'l' versus 'a' shows the maximum eccentricity achieved during the 1 million year integration of the fictitious Trojan. Instability was defined when -- due to the large eccentricity of the Trojan (e > 0.5) -- the area around the Lagrange point was definitely left. Left picture for Jupiter as the primary (m_2=m_Jupiter), right picture for a very massive primary (m_2 = 7 m_Jupiter). Comparing the different plot one can see how sensitive is the stable region with respect to the primaries' eccentricity AND its mass. Computations for less massive primaries -- down to the mass of Uranus -- did not change the stable area significantly in comparison with the one with the mass of Jupiter.

Name	Spectraltype	M_sun	M.sini [M_jup]	a [AU]	ecc.	HZ [AU]	partly in Hz [%]
HD 93083	K3V	0.70	0.37	0.48	0.14	0.4-1.3	100
HD 134987	G5V	1.05	1.58	0.78	0.24	0.75-1.40	58
HD 17051	G0V	1.03	1.94	0.91	0.24	0.70-1.30	100
HD 28185	G5	0.99	5.70	1.03	0.07	0.70-1.30	100
HD 108874	G5	1.00	1.65	1.07	0.20	0.70-1.30	100
HD 27442	K2IVa	1.20	1.28	1.18	0.07	0.93-1.80	100
HD188015	G5IV	1.08	1.26	1.19	0.15	0.70-1.60	100
HD 114783	K0	0.92	0.99	1.20	0.10	0.65-1.25	50
HD 20367	G0	1.05	1.07	1.25	0.23	0.75-1.40	76
HD 23079	(F8)/G0V	1.10	2.61	1.65	0.10	0.85-1.60	35

Tables of ESPs in which Trojan-like planets are stable: The upper table gives a summary of all systems with one discoverd planet and the lower table shows all possible Trojan-planet candidates in multiple extrasolar systems. For more examples see Dvorak et al., 2004,

Name	Spectraltype	M_sun	M.sini [M_jup]	a [AU]	ecc.	HZ [AU]	partly in HZ [%]	Resonances
Gliese 876 c	M4V	0.32	0.56	0.13	0.12	0.10 - 0.20	100	2:1
Gliese 876 b	M4V	0.32	1.89	0.21	0.27		0	
HD 82943 c	G0	1.05	0.88	0.73	0.54	0.75 - 1.40	68	2:1
HD 82943 b	G0	1.05	1.63	1.16	0.41	0.75 - 1.40	0	
HD 12661 b	G6V	1.07	2.30	0.83	0.35	0.80 - 1.45	60	11:2
HD 12661 c	G6V	1.07	1.57	2.56	0.2	0.80 - 1.45	0	
HD 160691 b	G3IV-V	1.08	1.67	1.48	0.31	0.85 - 1.60	44	3:1
HD 160691 c	G3IV-V	1.08	3.10	4.17	0.57	0.85 - 1.60	0	
HD 160691 d	G3IV-V	1.08	0.045	0.09	0.00	0.85 - 1.60	0	

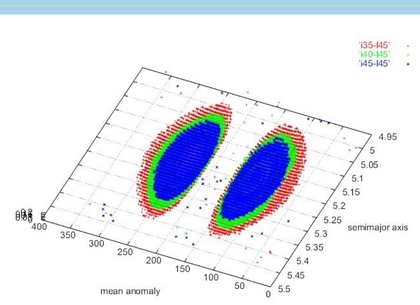

Figure 2: Stable region depending on the inclinations for the Jupitersystem as model for ESPs: In this plot one can see how the size of the stable region shrinks with the initial inclination of the fictitious planet in orbit around the Lagrangian equilibrium points. The grid was similar as the one for Fig.2; here we can also see that the size of the stable region around L4 and L5 is the same. In red we visualize the extension of the stable region for i=35, in green for i=40 and in blue for i=45 degrees; for inclinations up to the 30 degrees the size stays almost the same.

Stability Zones for S-type motion

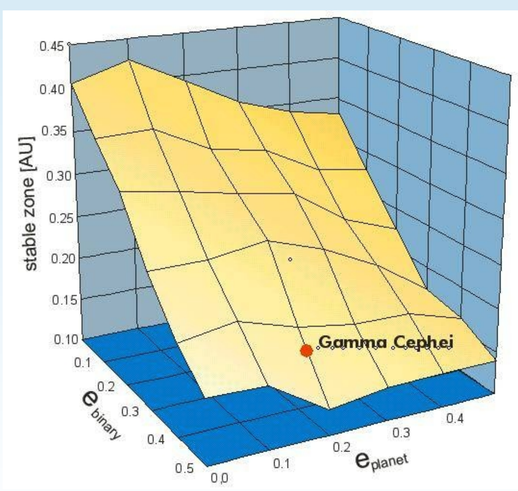

Figure 3: The size of the stable zone of S-type motion in a double star system with mass-ratio 0.2 depending on the eccentricities of the binary (between 0 and 0.5) and of the planet (between 0 and 0.5). It is clearly seen that an increase of the binary's eccentricity leads to a stronger reduction of the stable zone than an increase of the planet's eccentricity (for more details see Pilat-Lohinger & Dvorak, 2002, CMDA 82, p. 143). This study can be applied to the real binary system Gamma Cephei, where $e_{binary} = 0.44$ and $e_{planet}=0.2$ so that the border of the stable zone is at 0.17 AU (=3.6 AU in the double star system Gamma Cephei) (for more details see Dvorak et al. 2003, A&A, 398, L1).

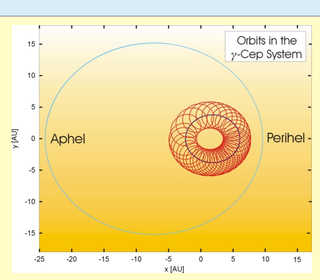

Figure 7: Orbits in the Gamma Cephei system (using the orbital parameters given by Cochran et al. 2002).

Acknowledgements:

E.P-L wants to acknowledge the support by the Austrian FWF - Hertha Firnberg project T122-N08. R.S. and B.F. want to acknowledge the support by the Austrian FWF - project no. P16024. The authors thank also the ÖAD projekt A12R04 (Dynamics of exoplanetary systems)

Stability catalogue of the HZ of ESPs

We show some examples of a catalogue of dynamical stability in the elliptic restricted three body problem (m_1: the star, m_2: the giant planet and m_3: a small terrestrial-like planet), where the configurations 1 and 2 described in the introduction are studied. The whole catalogue consist of 92 stability maps, for which the following initial conditions are used:

- semi-major axis of the giant planet: 1 (=unit of distance)
- eccentricity of the giant planet: between 0 and 0.5
- inclination, argument of peri-astron and node : 0
- degree mean anomaly: 0 or 180 degree

Test-planets:

- semi-major axis (inner case): between 0.1 and 0.9 (with a step of 10^{-3})
- semi-major axis (outer case): between 1.1 and 4.(with a step of 3.625×10^{-3})
- eccentricity, inclination, argument of peri-astron, node, mean anomaly: 0

For the stability study we used the 3 methods described in the introduction. All maps are dominated by mean motion resonances (MMR), that can represent either ordered (stable for infinite time) or weakly chaotic (which may become unstable after very long time) behavior. Due to the V-shape of MMRs in the (semi-major axis, eccentricity)-plane, resonances may overlap for high eccentricities so that chaotic motion occurs. For more details see Sandor et al. (2005, submitted to ApJ). How this map can be applied to spezial ESPs can be seen from the systems, that are inserted as examples.

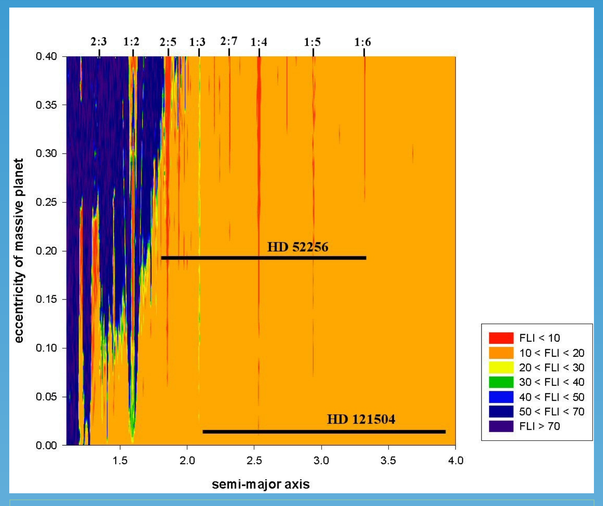

Figure 4a: Stability map computed by the FLIs for the outer case, when the mass-ratio=0.001 (Sun-Jupiter case) and the giant planet starts at the peri-center. Low values of the FLI label regular motion (red and range regions) and higher values indicate chaotic motion -- either weak (yellow and green regions) or strong chaotic (blue regions). The red stripes show stable resonant orbits.

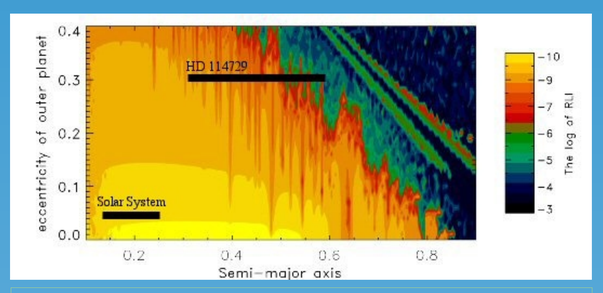

Figure 4b: Stability map computed by the RLI for the inner case, when the mass-ratio=0.001 and the giant planet starts at the peri-center. Like in fig. 1, regular motion is defined by low values of the RLIs (yellow and orange region) and chaotic motion is given by high values -- red and green regions indicate weak chaos and blue and black regions show the strong chaotic behavior. The RLI-plot is dominated by the different mean motion resonances. We have to note the peculiar feature in the chaotic region, where two almost parallel stripes of regular or weak chaotic motion are clearly visible and which indicate satellite-type orbits around the giant planet.

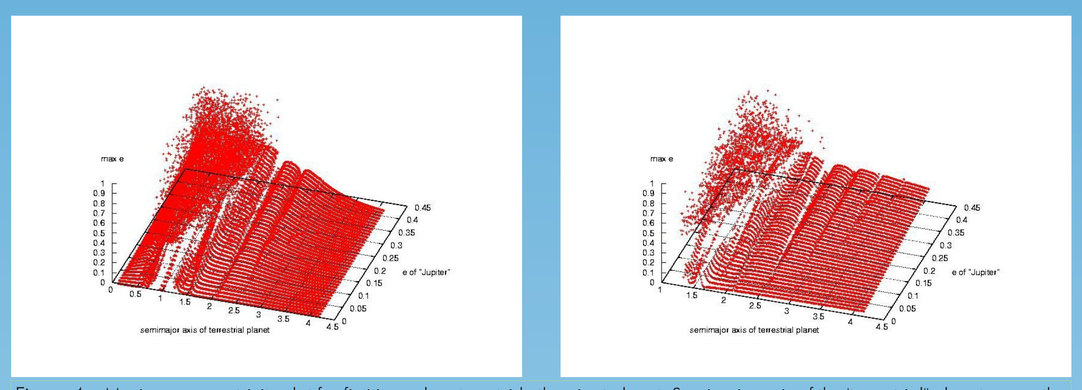

Figure 4c: Maximum eccentricity plot for fictitious planets outside the giant planet: Semimajor axis of the 'terrestrial" planet versus the eccentricity of the primary's orbit in the elliptic restricted three body problem. Close to the massive planet all orbits lead to escapes, then one can see that globally the eccentricities of the fictitious planet achieved during the 1 million year integration increases with large eccentrities of the primary. Well visible are the outer mean motion resonances 1:2, 1:3 and 1:4 on the left plot (for m_2=Jupiter) and also the high order resonances 1:5 and 1:6 for a 5 times more massive second primary and the same initial conditions.

Applications for real extrasolar systems

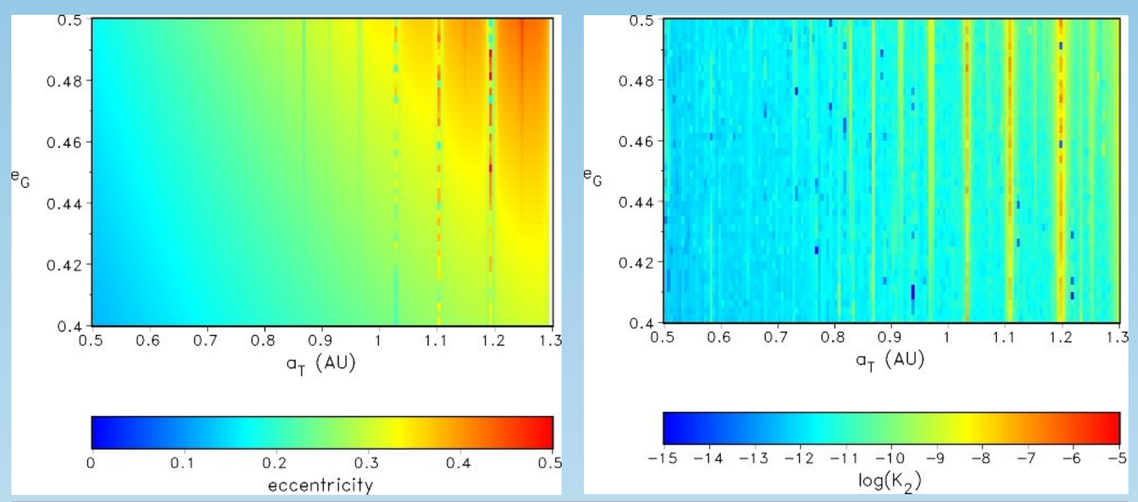

Figure 5: Initial condition diagramm for fictitious massless planets in the system Gl 777 (m_star=0.9 m_sun, m_planet=1.33 m_jupiter, semimajor axis a =4.8 AU, eccentricity e=0.48+/-0.2) for a grid of 80 x 80 in semimajor axes of the "terrestrial planet" versus e (of the giant). Because of the uncertainty in the eccentricity we used different initial eccentricities of the giant planet. The initial orbit of the fictitious planet was always circular, the initial angles were set to 0. The colors indicate the maximum achieved eccentriicty during the integration of 1 million years on the left graph. Using the same data of the numerical integration we determined via reccurence plots the Renyi entropie, a measure of chaos which is equivalent to the Lyapunov exponents (right graph). As in the left plot blue color means quasiperiodic motion, red color indicates chaotique motion. We find in both plots a very similar structure of vertical stripes due high order mean motion resonances. The entropy plot shows many more resonances and the left plot clearly visualizes that the inner part of the habitable zone (0.75 -- 1.25 AU) -- where water may be in liquid form -- allows motions for additional planets on low eccentric orbits.

Figure 6: shows the habitable zone (green region) and the planets of some selected extrasolar planetary systems. Additional the perihelion of the known planets, according to their eccentricity is shown (red region). For more details see Asghari et al., 2004, A&A, 426, p.353.